Singlet oxygen-induced alteration of bacteria associated with phytodetritus: Effect of irradiance

Christopher Burot, Patricia Bonin, Gwénola Simon, Laurie Casalot, Jean-françois Rontani

Singlet oxygen-induced alteration of bacteria associated with phytodetritus: effect of irradiance

Journal:	*Journal of Phycology*
Manuscript ID	JPY-22-138-ART.R2
Manuscript Type:	Research Article
Date Submitted by the Author:	n/a
Complete List of Authors:	Burot, Christopher; Mediterranean Institute of Oceanography Bonin, Patricia; Mediterranean Institute of Oceanography simon, Gwenola; Mediterranean Institute of Oceanography Casalot, Laurie; Mediterranean Institute of Oceanography Rontani, Jean-François; Mediterranean Institute of Oceanography
Keywords:	algae, light, molecular
Alternate Keywords:	Senescent phytoplankton, Attached bacteria, Type-II photosensitized oxidation, Irradiance effect, Arctic, Sinking particulate matter, Sea ice

Singlet oxygen-induced alteration of bacteria associated with phytodetritus: effect of irradiance

Burot Christopher, Bonin Patricia, Simon Gwénola, Casalot Laurie, Rontani Jean-François*

Aix-Marseille University, Université de Toulon, CNRS/INSU/IRD, Mediterranean Institute of Oceanography (MIO), UM 110, 13288 Marseille, France.

* Corresponding author: jean-francois.rontani@mio.osupytheas.fr

Abstract. Contrasting irradiation of senescent cells of the diatom *Thalassiosira* sp. in association with the bacterium *Pseudomonas stutzeri* showed the effect of intensity of irradiance on the transfer of singlet oxygen ($^1O_2$) to bacteria attached to phytoplanktonic cells. Under low irradiances, $^1O_2$ is produced slowly, favors the oxidation of algal unsaturated lipids (photodynamic effect) and limits $^1O_2$ transfer to attached bacteria. However, high irradiances induce a rapid and intense production of $^1O_2$, which diffuses out of the chloroplasts and easily reaches the attached bacteria, where it efficiently oxidizes their unsaturated membrane components. Analysis of numerous sinking particle samples collected in different regions of the Canadian Arctic showed that the photooxidation state of attached bacteria increased from ice-covered areas to open water, in agreement with *in vitro* results. Photooxidation of bacteria appeared to be particularly intense in sea ice, where the sympagic algae–bacteria association is maintained at relatively high irradiances for long periods of time.

Keywords. Senescent phytoplankton; Attached bacteria; Type II photosensitized oxidation; Irradiance effect; Arctic; Sinking particulate matter; Sea ice.

1. Introduction

Type II photooxidation processes are light-induced indirect degradation reactions, that involve the action of a photosensitizer molecule (typically pigments or aromatic compounds) in its triplet state (Gollnick, 1968). Chlorophyll, which is an efficient photosensitizer (Foote, 1976), can trigger type II photooxidation processes in phytoplanktonic cells, especially in late bloom phases when they are senescent (Nelson, 1993). Indeed, in senescent cells, the cessation of photosynthetic reactions results in an accelerated rate of formation of ^{3}Chl and reactive oxygen species (ROS), mainly singlet oxygen ($^1O_2$) (Knox and Dodge, 1985; Nelson, 1993). The rate of formation of these potentially damaging species can then exceed the quenching capacity of the photoprotective system, thus enabling the photodegradation of cell components (photodynamic effect) to occur (Merzlyak and Hendry, 1994). $^1O_2$ reacts with a broad range of cellular compounds but especially unsaturated lipids such as sterols and unsaturated fatty acids (Rontani and Belt, 2020), proteins (Morgan et al., 2004) and nucleic acids (Agnez-Lima et al., 1999; Ravanat et al., 2000). The very high reactivity of $^1O_2$ with these biomolecules is due to the lack of spin restriction that normally prevents $^3O_2$ from reacting with these compounds (Zolla and Rinalducci, 2002).

The $^1O_2$ thus formed reacts not only with membrane components of phytoplankton but also with the monounsaturated fatty acids (MUFAs) of its neighboring attached bacteria (Rontani et al., 2003; Christodoulou et al., 2010, Petit et al., 2013, 2015). Indeed, in phototrophic cells, the radius of the sphere of activity of $^1O_2$ from its point of production was estimated to be between 155 and 340 nm (Baier et al., 2005; Ogilby, 2010; Skovsen et al., 2005), which is a sufficient distance to allow it to cross the cellular membranes (Ogilby, 2010) and thus attack attached bacteria.

It has previously been demonstrated that low solar irradiance favors slow production and diffusion of $^1O_2$ through the membranes and thus increases photooxidative damage of

the unsaturated algal lipids (Amiraux et al., 2016). However, the effects of intensity of solar irradiance on the photooxidation of bacteria attached to phytodetritus are totally unknown.

Here, to clarify this issue, we incubated senescent cells of the diatom *Thalassiosira* sp. (a phytoplankton genus widely distributed in oceans, Malviya et al., 2016) in association with the bacteria *Pseudomonas stutzeri* under contrasted artificial light irradiances. Bacteria of the *Pseudomonas* genus were selected because they are often associated with *Thalassiosira* cells (Bidle and Azam, 2001; Schaum, 2019). To validate the results, we compared the photooxidation state of diatoms and their attached bacteria in numerous samples of Arctic sea ice and sinking particulate matter. Samples were collected at different depths under open water. marginal ice zone and first-year ice).

2. Material and methods

2.1 Collection of in situ samples

Detailed descriptions of the Arctic marine particulate matter and sea ice sample collection processes (e.g. sampling dates, depths, volumes, etc.) can be found in Rontani et al. (2012, 2016, 2022) and Amiraux et al. (2020). Briefly, sinking particles were collected i) in Resolute Passage under first-year ice at 5 m and 30 m depth with Hydro-Bios MS12-model multi-sediment traps (Rontani et al., 2016), ii) in central Baffin Bay under the marginal ice zone at 25 m depth with a Technicap PPS4 drifting sediment trap (Rontani et al., 2022), and iii) in the Beaufort Sea in open water at 100 m depth with Technicap PPS traps (Rontani et al., 2012). Sea-ice samples were collected at GreenEdge Project landfast ice station located near Broughton Island in the Davis Strait using a Kovacs Mark V 14-cm-diameter corer and focusing on the bottommost 10 cm of sea ice (Amiraux et al., 2020) (Fig. 1).

94

95 *2.2. Algal phytodetritus production*

96 The non-axenic diatom *Thalassiosira* sp. RCC1714 was obtained from the Roscoff
97 culture collection. Diatoms were grown in F/2 medium at 17°C in a constant-environment
98 cabinet under an irradiance of 18 $W.m^{-2}$ (Osram, Lumilux 12:12h light/dark cycle). After
99 two months of growth, cell density was measured by counting under microscope, and death
100 of the algal cells was induced by sonication. *Thalassiosira* sp. cells were sonicated on ice
101 using a Branson Sonifier 450 ultrasound generator equipped with a Branson S450A cell
102 disruptor probe at 240 W for 10 minutes (duty cycle 50%). The sonicated cells were then
103 sub-sampled in 50 mL Falcon tubes and stored at -20°C for later photooxidation
104 experiments.

105

106 *2.3. Culturing of P. stutzeri*

107 Pre-culture of *P. stutzeri* ATCC 14405 was grown aerobically overnight on a rotary
108 shaker in the dark at 17°C on marine broth medium (US Biological™) diluted 1:10 with
109 sterilized artificial sea water (Kester et al., 1967) therefore not adding large amounts of
110 assimilable organic matter from the inoculum in the further steps. The culture was inoculated
111 with the aerobic pre-culture to obtain an initial OD_{620nm}, about 0.020. At the mid growth
112 exponential phase, the incubation was stopped and cells counted based on epifluorescence
113 in the presence of fluorochrome (4P,6-diamidino-2P-phenylindole dihydrochloride, DAPI)
114 as described in Otto (1990).

115

116 *2.4. Photooxidation experiments*

117 Phytodetritus and bacteria were mixed (ratio algal:bacterial cells = 1:5) in K medium
118 (Keller et al., 1987) to obtain a final volume of 100 mL. The experiments were performed in

triplicate. After taking three 10 mL sub-samples (controls before irradiation) the reactional systems were exposed to high or low irradiance.

2.4.1. *High irradiance experiments*

The high-irradiance experiments were carried out in sterilized quartz and glass tubes (100 mL) with an Altas Suntest CPS + solar simulator equipped with a Xenon NXE 1500 lamp producing a high solar irradiance (500 $W.m^{-2}$) in the 300–800 nm range, i.e. close to that generally observed at noon at the surface of the Mediterranean Sea (Sarra et al., 2019) and not far from the one observed at the surface of Arctic waters in summer (up to 350 W m^{-2}, Horvat et al., 2020). To eliminate UV radiation, experiments were also performed in glass tubes reducing the irradiance to 446 $W.m^{-2}$. After irradiation with a light dose of 1000 $KJ.m^{-2}$ (corresponding to an irradiation time of 0.5 and 15 h at the surface and at the deep chlorophyll maximum (DCM) of the Mediterranean Sea, respectively), 10 mL was collected. All the samples were filtered on 0.8 µm glass fiber filters (GF/F) to concentrate bacteria attached on phytodetritus and stored at -20°C until further lipid extraction.

Controls were also conducted in triplicate with no phytodetritus. Bacteria (*P. stutzeri*) were mixed with sterilized artificial sea water complemented with 0.1 $g.L^{-1}$ of lactate/acetate (50:50) as carbon source, in 100 mL sterilized quartz or glass tubes and exposed to light in the solar simulator for the same duration as the tubes containing phytodetritus and bacteria. After irradiation, 50 mL was sampled and bacteria were concentrated by centrifugation (Beckman & Coulter Allegra X-22 centrifuge at 20,000 *g* for 30 min). The irradiated bacterial cells were then stored at -20°C until further lipid extraction.

2.4. 2. *Low irradiance experiments*

Low-irradiance photosynthetically active radiation (PAR) (18 $W.m^{-2}$) in the range 400–750 nm, i.e. comparable to that observed at the DCM in the Mediterranean Sea (Maraňón et al., 2020), was obtained with a Binder incubator equipped with Osram Lumilux lamps. The vials were exposed to a light dose of 1000 $KJ.m^{-2}$ in the incubator at 17°C. After irradiation, 10 mL samples was collected, filtered on 0.8 µm GF/F and stored at -20°C until further lipid extraction. Control experiments without phytodetritus were also carried out as described above.

2.5. Lipid extraction and derivatization

Samples (GF/F filters or bacterial pellets) were reduced with excess $NaBH_4$ after adding MeOH (25 mL, 30 min) to reduce labile hydroperoxides (resulting from photooxidation) to alcohols, which are more amenable to gas chromatography-mass spectrometry (GC-MS) analysis. Water (25 mL) and KOH (2.8 g) were then added and the resulting mixture was saponified by refluxing (2 h), then cooled, acidified (HCl, 2 N) to pH 1, and extracted with dichloromethane (3 × 20 mL). The combined extracts were then concentrated by rotary evaporation at 40°C to give total lipid extracts (TLEs).

Dry TLEs were derivatized by dissolving them in 300 µL of a mixture of pyridine/bis-(trimethylsilyl)trifluoroacetamide (BSTFA; Supelco; 2:1, v/v) and silylated in a heating block (50°C, 1 h). After evaporation to dryness under a stream of N_2, the derivatized residue was dissolved in ethyl acetate/BSTFA (to avoid desilylation) and analyzed by GC-MS/MS.

2.6. *Gas chromatography-tandem mass spectrometry (GC-MS/MS)*

GC-MS/MS analyses were performed on an Agilent 7890A/7010A tandem-quadrupole gas chromatograph system (Agilent Technologies, Les Ulis, France) using a cross-linked 5% phenyl-methylpolysiloxane (Agilent; HP-5MS ultra inert, 30 m × 0.25 mm, 0.25 µm film

thickness) capillary column. Analyses were performed with an injector operating in pulsed splitless mode set at 270°C. Oven temperature was ramped from 70°C to 130°C at 20°C.min^{-1}, then to 250°C at 5°C.min^{-1} and finally to 300°C at 3°C.min^{-1}. Pressure of the carrier gas (He) was maintained at 0.69×10^5 Pa until the end of the temperature program, then ramped from 0.69×10^5 Pa to 1.49×10^5 Pa at 0.04×10^5 Pa.min^{-1}. The following mass spectrometer conditions were used: electron energy 70 eV, source temperature 230°C, quadrupole 1 temperature 150°C, quadrupole 2 temperature 150°C, collision gas (N_2) flow 1.5 mL.min^{-1}, quench gas (He) flow 2.25 mL.min^{-1}, mass range 50–700 Daltons, cycle time 313 ms. Vaccenic acid photooxidation products were quantified in multiple reaction monitoring (MRM) mode using the transitions *m/z* 339 → 131 for the parent vaccenic acid and *m/z* 199 → 129, *m/z* 213 → 129, *m/z* 357 → 129 and *m/z* 371 → 129 for its oxidation products (Rontani, 2021). Precursor ions were selected from the most intense ions and specific fragmentations observed in electron ionization (EI) mass spectra. Collision-induced dissociation (CID) was optimized by using collision energies at 5, 10, 15 and 20 eV. Quantification involved peak integration and determination of individual response factors using standard compounds and Mass Hunter software (Agilent Technologies, Les Ulis, France).

2.7. Standard compounds

Vaccenic and palmitoleic acids were obtained from Sigma-Aldrich. Vaccenic acid oxidation was achieved using Fe^{2+}/ascorbate (Loidl-Stahlhofen and Spiteller, 1994). Subsequent reduction of the resulting hydroperoxides in methanol with excess $NaBH_4$ afforded the corresponding hydroxyacids.

2.8. Statistical analysis

193 Results of statistical tests were considered to be significant at a confidence level of
194 95% ($\alpha = 0.05$). All tests were performed using XL-Stat Statistics software.
195
196 **3. Results and Discussion**
197
198 *3.1. In vitro experiments*
199 To determine the effect of solar irradiance on the efficiency of transfer of $^1O_2$ from
200 phytodetritus to their attached bacteria, senescent *Thalassiosira* sp. cells associated with *P.*
201 *stutzeri* were irradiated by a light dose of 1000 KJ.m^{-2} under contrasting irradiances, i.e. 18
202 (PAR), 446 (PAR) and 500 (UV+PAR) W.m^{-2}. The efficiency of $^1O_2$ transfer to bacteria was
203 estimated based on the measured concentration of photooxidation products of vaccenic acid
204 (pmol.L^{-1}). Vaccenic acid was present in high proportion in *P. stutzeri* (Rainey et al., 1994)
205 but only in weak amount in the unknown bacterial community associated with the non-
206 axenic strain of *Thalassiosira* sp. employed (amount estimated to be more than one order of
207 magnitude lesser than this present in the cells of *P. stutzeri* added during the different
208 experiments).
209 Type-II photosensitized oxidation of vaccenic acid involves the addition of $^1O_2$ to the
210 two carbon atoms of its Δ^{11} double bond, and leads to the formation of 11-
211 hydroperoxyoctadec-12(*trans*)-enoic and 12-hydroperoxyoctadec-10(*trans*)-enoic acids
212 (Rontani, 2021). These hydroperoxides can subsequently undergo stereoselective radical
213 allylic rearrangement to afford 13-hydroperoxyoctadec-11(*trans*)-enoic and 10-
214 hydroperoxyoctadec-11(*trans*)-enoic acids, respectively (Porter et al., 1995). *Trans* allylic
215 hydroxy acids arising from $NaBH_4$ reduction of these hydroperoxyacids are sufficiently
216 stable for use as tracers of type-II photosensitized oxidation processes (Marchand and
217 Rontani, 2001).

Interestingly, we detected only trace amounts of vaccenic acid photooxidation products before irradiation (under the detection limit) and in the different controls carried out without algae (Table 1, Fig. 2). Significant increases of vaccenic acid photooxidation products were observed with algae amendment after 0.5 and 15H for low and high irradiance respectively (Wilcoxon test, n=6, $p=0.031<0.05$). As previously observed (Rontani et al., 2003; Petit et al., 2015), photooxidation of heterotrophic bacteria membranes requires the presence of senescent phytoplankton cells. Our results showed a strong effect of intensity of irradiance on the photooxidation of the bacterial membranes (Table 1, Fig. 2). Indeed, the concentration of vaccenic acid photooxidation products reached 2741 ± 21 $nmol.L^{-1}$ under high PAR irradiance but only 464 ± 190 $nmol.L^{-1}$ under low irradiance (Fig. 2). The highest concentration of vaccenic acid oxidation products (3998 ± 1010 $nmol.L^{-1}$) was observed under high UV+PAR irradiance (Table 1, Fig. 2) and may be attributed to the presence of additional UV radiations. In phytodetritus, chlorophyll can act as photosensitizer not only under PAR (Nelson, 1993) but also under UV (Ying He and Häder, 2002), since they absorb in the UV range (Queseda and Vincent, 1997; Ehling-Schulz and Scherer, 1999). This assumption is well supported by the profile of photooxidation products obtained under these conditions, showing the presence of a high proportion of allylic 11- and 12-hydroxyacids with a cis double bond (Fig. S1) typical of the UV-induced photooxidation of MUFAs (Christodoulou et al., 2010).

Amiraux et al. (2016) previously showed in senescent diatom cells that low irradiances induce a slow but long-lasting production of $^1O_2$ that strongly oxidizes algal unsaturated lipids and sterols, through a process called “photodynamic effect” (Knox and Dodge, 1985; Skovsen et al., 2005), whereas high irradiances lead to stronger but shorter production of $^1O_2$ that strongly photooxidizes the sensitizer (chlorophyll) through a process called “photobleaching” but with only a weak photodynamic effect (Amiraux et al., 2016; Rontani

et al., 2021). This effect of the intensity of solar irradiance on the efficiency of the photodynamic effect in senescent phytoplankton cells was then confirmed *in situ* (Rontani et al., 2021).

The effect of irradiance on the efficiency of photooxidation of attached bacteria thus appears to be exactly the opposite of the effect on phytoplankton. Under low irradiance, the low flux of $^1O_2$ produced reacts with the unsaturated membrane components of phytodetritus and thus gets quenched before it reaches attached bacteria (Fig. 3). In contrast, under strong irradiance, a higher proportion of $^1O_2$ is efficiently transferred to the attached bacteria, strongly oxidizing their unsaturated lipids (Fig. 3). This new concept opens interesting perspectives in the study of phytoplankton-bacteria relationships.

3.2. Confirmation of the results obtained in vitro in samples collected in situ

To confirm the enhancement of the efficiency of photooxidation processes on bacteria attached to phytoplankton cells, we analyzed a variety (n=58) of sinking particulate matter and sea ice samples collected in the Arctic (Fig. 1), where irradiance at the sea ice–water interface and in the water column varies strongly according to the albedo of snow and ice and to snow and ice thickness (Chresten Lund-Hansen et al., 2021). Sinking particulate matter samples were collected: (i) in summer at 100 m in open water in the Beaufort Sea (Rontani et al., 2012), (ii) in summer at 25 m in the marginal ice zone of central Baffin Bay (Rontani et al., 2022), and (iii) in spring at 5 m and 30 m in ice-covered Resolute Passage (Rontani et al., 2016). Sea-ice samples (0–10 cm) were collected in spring during the GreenEdge campaign at Qikiqtarjuaq (Baffin Bay, Arctic Ocean; Amiraux et al., 2020). To compare the efficiency of type-II photooxidation processes in algal and bacterial material, we used the ratio of % vaccenic acid photooxidation to % palmitoleic acid photooxidation. Vaccenic acid is generally considered to be specific to bacteria (Lambert and Moss, 1983;

268 Sicre et al., 1988), whereas palmitoleic acid is the main fatty acid component of sympagic
269 diatoms (Fahl and Kattner, 1993; Falk-Petersen et al., 1998; Leu et al., 2010). Although
270 palmitoleic acid is also present in several bacteria (e.g. de Carvalho and Caramujo, 2014),
271 the contribution of bacteria to palmitoleic acid in the samples analyzed (dominated by
272 diatoms) is negligible relative to the contribution of sympagic algae.

273 The results obtained show higher % vaccenic acid photooxidation/% palmitoleic
274 photooxidation ratios in sinking particles collected in open-water Beaufort Sea than in ice-
275 covered Resolute Passage (Fig. 4A). This difference may be attributed to the mean PAR
276 irradiance in the mixed surface layer, which is considerably higher in open water than in ice-
277 covered zones (e.g. 365 ± 62 and 10.9 ± 2.7 µmol photons.m^{-2}.s^{-1} during the spring-summer
278 transition in Beaufort Sea, respectively; Alou-Font et al., 2016). The ratios observed in the
279 Baffin Bay marginal ice zone (where ice concentration ranges from 15% to 80%) were
280 logically intermediate (Fig. 4A). The decrease in the ratio observed between 5 and 30 m in
281 the Resolute Passage (Fig.4A) could be attributed to the presence in the deeper trap of highly
282 aggregated senescent sea-ice algae settling sufficiently rapidly out of the euphotic zone to
283 avoid significant photooxidation (Rontani et al., 2016), however these differences were not
284 significant (p-value > 0.05, see Fig. 4A, Table S1).

285 Very high ratios were found in the bottommost 10 cm of sea ice collected at the
286 GreenEdge ice camp in 2016 (Fig. 4B). Under 75 cm of sea ice, irradiance can reach 105.9
287 µmol photons m^{-2}.s^{-1} without snow cover and decrease to 51.9 µmol photons m^{-2}.s^{-1} with a
288 snow cover of 1 cm (Lund-Hansen et al., 2021). In this solid habitat, the bacteria–sympagic
289 algae association may thus be maintained at relatively high irradiances during long periods,
290 these conditions strongly favoring the photooxidation of bacteria. It was previously
291 demonstrated that during the early stages of ice melt, sympagic bacteria undergo an intense
292 osmotic stress in hypersaline ice brines (Amiraux et al., 2017) and are affected later in the

season by the release of bactericidal free palmitoleic acid by sympagic algae under the effect of light stress (Amiraux et al., 2020). Our results show that these organisms may also undergo a strong photooxidative stress in the ice resulting from a strong and efficient transfer of $^1O_2$ from senescent sympagic algae. These different stresses are thought to strongly decrease the mineralization potential of bacteria attached to ice algae and thus favor the preservation of sympagic material in Arctic sediments (Amiraux et al., 2021; Rontani et al., 2022).

4- Conclusion

Incubation of senescent cells of the diatom *Thalassiosira* sp. associated with the bacteria *P. stutzer*i under contrasting artificial light irradiances made it possible to demonstrate that high irradiances strongly favor photooxidation of the unsaturated membrane components of bacteria attached to senescent phytoplankton cells. Under these conditions, only a small part of $^1O_2$ produced in chloroplasts reacts with membrane components of senescent algae, and so the remainder is efficiently transferred to their attached bacteria, inducing strong oxidative damage. Conversely, low irradiances favor photooxidation of the unsaturated algal lipids rather than attached bacteria. Indeed, $^1O_2$ slowly generated under these conditions reacts with unsaturated lipids of the algal cells and is thus quenched before it can reach bacterial membranes. These findings were also confirmed *in situ*, where we observed the same tendencies in a variety of Arctic environmental samples (sea ice and sinking particulate matter). The transfer of $^1O_2$ from senescent algae to their attached bacteria appeared to be particularly efficient in sea ice where the sympagic algae–bacteria association is maintained at relatively high irradiances during long periods of time.

Acknowledgements

Sediment trap samples from the Beaufort Sea were obtained through the Long-Term Oceanic Observatories Program led by ArcticNet–Network of Centers of Excellence (NCE) of Canada. The collection of sinking particles from Resolute Passage was supported through a University of Manitoba start-up grant and the Natural Sciences and Engineering Research Council of Canada (NSERC). Sinking particles and sea ice samples from Baffin Bay were collected in the framework of the GreenEdge project funded by the following French and Canadian programs and agencies: ANR (Contract #111112), CNES (project #131425), IPEV (project #1164), CSA, Fondation Total, ArcticNet, LEFE, and the French Arctic Initiative. The project was conducted with scientific coordination by the Canada Excellence Research Chair on Remote sensing of Canada's New Arctic Frontier and the CNRS/Université Laval Takuvik joint international laboratory (UMI3376). We thank Québec-Ocean, the CCGS Amundsen, and the Polar Continental Shelf Program for their in-kind contribution to polar logistics and scientific equipment, and the European Regional Development Fund (ERDF) project Oceanomed (No. 1166-39417) for funding the GC-MS/MS system employed. Thanks are also due to two anonymous reviewers for their very useful and constructive comments.

References

Agnez-Lima, L. F., Mascio, P. D., Napolitano, R. L., Fuchs, R. P., & Menck, C. F. M. 1999. Mutation Spectrum Induced by Singlet Oxygen in *Escherichia coli* Deficient in Exonuclease III. *Photochem. Photobiol*. 70(4): 505-511.

Alou-Font, E., Roy, S., Agustí, S., & Gosselin, M. 2016. Cell viability, pigments and photosynthetic performance of Arctic phytoplankton in contrasting ice-covered and

343 open-water conditions during the spring–summer transition. *Mar. Ecol. Prog. Ser.*
344 543: 89-106.
345 Amiraux, R., Jeanthon, C., Vaultier, F., & Rontani, J.-F. 2016. Paradoxical effects of
346 temperature and solar irradiance on the photodegradation state of killed phytoplankton.
347 *J. Phycol*. 52(3): 475-485.
348 Amiraux, R., Belt, S. T., Vaultier, F., Galindo, V., Gosselin, M., Bonin, P., & Rontani, J.-F.
349 2017. Monitoring photo-oxidative and salinity-induced bacterial stress in the Canadian
350 Arctic using specific lipid tracers. *Mar. Chem*. 194: 89-99.
351 Amiraux, R., Burot, C., Bonin, P., Massé, G., Guasco, S., Babin, M., Vaultier, F., & Rontani,
352 J.-F. 2020. Stress factors resulting from the Arctic vernal sea-ice melt: Impact on the
353 viability of bacterial communities associated with sympagic algae. *Elementa: Sci.*
354 *Anthr*. 8(1): 076.
355 Amiraux R., Bonin P., Burot C. & Rontani J.-F. 2021. Use of stress signals of their attached
356 bacteria to monitor sympagic algae preservation in Canadian Arctic sediments.
357 *Microorganisms* 9: 2626.
358 Baier, J., Maier, M., Engl, R., Landthaler, M., & Bäumler, W. 2005. Time-resolved
359 investigations of singlet oxygen luminescence in water, in phosphatidylcholine, and in
360 aqueous suspensions of phosphatidylcholine or HT29 cells. *J. Phys. Chem. B*, 109(7):
361 3041-3046.
362 Bidle, K. D. & Azam, F. 2001. Bacterial control of silicon regeneration from diatom detritus:
363 significance of bacterial ectohydrolases and species identity. *Limnol. Oceanogr.*
364 46(7) : 1606-1623.
365 Christodoulou, S., Joux, F., Marty, J.-C., Sempéré, R., & Rontani, J.-F. 2010. Comparative
366 study of UV and visible light induced degradation of lipids in non-axenic senescent
367 cells of *Emiliania huxleyi. Mar. Chem*. 119(1): 139-152.

de Carvalho, C. C. & Caramujo, M. J. 2014. Bacterial diversity assessed by cultivation-based techniques shows predominance of *Staphylococccus* species on coins collected in Lisbon and Casablanca. *FEMS Microbiol. Ecol*. 88(1): 26-37.

Ehling-Schulz, M., & Scherer, S. 1999. UV protection in cyanobacteria. Eur. J. Phycol. 34(4): 329-338.

Fahl, K., & Kattner, G. 1993. Lipid Content and fatty acid composition of algal communities in sea-ice and water from the Weddell Sea (Antarctica). *Polar Biol*. 13(6): 405-409.

Falk-Petersen, S., Sargent, J. R., Henderson, J., Hegseth, E. N., Hop, H., & Okolodkov, Y. B. 1998. Lipids and fatty acids in ice algae and phytoplankton from the Marginal Ice Zone in the Barents Sea. *Polar Biol*. 20(1): 41-47.

Foote, C. S. 1976. Photosensitized oxidation and singlet oxygen: Consequences in biological systems. *In* W. A. Pryor [Ed.] *Free Radicals in Biology*, Vol II. Academic Press, New York, 35, 3-22.

Gollnick, K. 1968. Type II Photooxygenation Reactions in Solution. *In* W. A. Noyes, G. S. Hammond, & J. N. Pitts [Eds.] *Advances in Photochemistry.* John Wiley & Sons, Inc. 1-122.

He, Y. Y., & Häder, D. P. 2002. UV-B-induced formation of reactive oxygen species and oxidative damage of the cyanobacterium *Anabaena* sp.: protective effects of ascorbic acid and N-acetyl-L-cysteine. *J. Photochem. Photobiol. B: Biol.* 66(2): 115-124.

Horvat, C., Flocco, D., Rees Jones, D. W., Roach, L., & Golden, K. M. 2020. The Effect of Melt Pond Geometry on the Distribution of Solar Energy Under First-Year Sea Ice. *Geophys. Res. Let*. 47(4), e2019GL085956.

Keller, M. D., Selvin, R. C., Claus, W., & Guillard, R. R. L. 1987. Media for the culture of oceanic ultraphytoplankton. *J. Phycol*. 23: 633-8.

392 Kester, D. R., Duedall, I. W., Connors, D. N., & Pytkowicz, R. M. 1967. Preparation of
393 Artificial Seawater. *Limnol. Oceanogr.* 12(1): 176-179.
394 Knox, J. P., & Dodge, A. D. 1985. Singlet oxygen and plants. *Phytochemistry* 24(5): 889-
395 896.
396 Lambert, M. A., & Moss, C. W. 1983. Comparison of the effects of acid and base hydrolyses
397 on hydroxy and cyclopropane fatty acids in bacteria. *J. Clin. Microbiol*. 18(6), 1370-
398 1377.
399 Leu, E., Wiktor, J., Søreide, J., Berge, J., & Falk-Petersen, S. 2010. Increased irradiance
400 reduces food quality of sea ice algae. *Mar. Ecol. Progr. Ser*. 411: 49-60.
401 Loidl-Stahlhofen, A., Hannemann, K., & Spiteller, G. 1994. Generation of α-
402 hydroxyaldehydic compounds in the course of lipid peroxidation. *Biochim. Biophys.*
403 *Acta (BBA) - Lipids and Lipid Metabolism*, 1213(2): 140-148.
404 Lund-Hansen, L. C., Bjerg-Nielsen, M., Stratmann, T., Hawes, I., & Sorrell, B. K. 2021.
405 Upwelling Irradiance below Sea Ice - PAR Intensities and Spectral Distributions. *J.*
406 *Mar. Sci. Eng.* 9(8): 830.
407 Malviya, S., Scalco, E., Audic, S., Vincent, F., Veluchamy, A., Poulain, J., Wincker, P.,
408 Iudicone, D., Colomban de Vargas, Bittner, L., Zingone, A. & Bowler, C. 2016.
409 Insights into global diatom distribution and diversity in the world's ocean. *Proc. Nat.*
410 *Acad. Sci.* 113(11): E1516-E1525.
411 Marañón, E., Van Wambeke, F., Uitz, J., Boss, E. S., Dinasquet, J., Engel, A., Haëntjens,
412 N., Perez-Lorenzo, M., Taillandier, V. & Zäncker, B. (2020). Deep maxima of
413 phytoplankton biomass, primary production and bacterial production in the
414 Mediterranean Sea during late spring, *Biogeosci. Discuss*. 1-28.

415 Marchand, D. & Rontani, J.-F. 2001. Characterisation of photooxidation and autoxidation
416 products of phytoplanktonic monounsaturated fatty acids in marine particulate matter
417 and recent sediments. *Org. Geochem*. 32: 287-304.
418 Merzlyak, M.N. & Hendry, G.A.F. 1994. Free radical metabolism, pigment degradation and
419 lipid peroxidation in leaves during senescence. *Proc. Royal Soc. Edinburgh* 102B:
420 459-471.
421 Morgan, P. E., Dean, R. T., & Davies, M. J. 2004. Protective mechanisms against peptide
422 and protein peroxides generated by singlet oxygen. *Free Rad. Biol. Med*. 36(4): 484-
423 496.
424 Nelson, J. R. 1993. Rates and possible mechanism of light-dependent degradation of
425 pigments in detritus derived from phytoplankton. *J. Mar. Res.* 51(1): 155-179.
426 Ogilby, P. R. 2010. Singlet oxygen: there is indeed something new under the sun. *Chem.*
427 *Soc. Rev*. 39(8): 3181-3209.
428 Otto, F. 1990. DAPI staining of fixed cells for high-resolution flow cytometry of nuclear
429 DNA. *In* Z. Darzynkiewicz & H. A. Crissman [Eds.] *Methods in Cell Biology.*
430 Academic Press. Vol. 33, pp. 105-110.
431 Petit, M., Sempéré, R., Vaultier, F., & Rontani, J.-F. 2013. Photochemical Production and
432 Behavior of Hydroperoxyacids in Heterotrophic Bacteria Attached to Senescent
433 Phytoplanktonic Cells. *Intern. J. Mol. Sci.* 14(6): 11795-11815.
434 Petit, M., Suroy, M., Sempere, R., Vaultier, F., Volkman, J. K., Goutx, M., & Rontani, J.-F.
435 2015. Transfer of singlet oxygen from senescent irradiated phytoplankton cells to
436 attached heterotrophic bacteria: Effect of silica and carbonaceous matrices. *Mar.*
437 *Chem*. 171: 87-95.
438 Porter, N. A., Caldwell, S. E., & Mills, K. A. 1995. Mechanisms of free radical oxidation of
439 unsaturated lipids. *Lipids* 30: 277-290.

Quesada, A., & Vincent, W. F. 1997. Strategies of adaptation by Antarctic cyanobacteria to ultraviolet radiation. *Eur. J. Phycol*. 32(4): 335-342.

Rainey, P. B., Thompson, I. P., & Palleroni, N. J. 1994. Genome and fatty acid analysis of *Pseudomonas stutzeri. Intern. J. Syst. Evol. Microbiol*. 44(1): 54-61.

Ravanat, J.-L., Di Mascio, P., Martinez, G. R., Medeiros, M. H. G., & Cadet, J. 2000. Singlet Oxygen Induces Oxidation of Cellular DNA. *J. Biol. Chem*. 275(51): 40601-40604.

Rontani, J.-F., Koblížek, M., Beker, B., Bonin, P., & Kolber, Z. S. 2003. On the origin of *cis*-vaccenic acid photodegradation products in the marine environment. *Lipids*, 38(10): 1085-1092.

Rontani, J.-F., Charriere, B., Forest, A., Heussner, S., Vaultier, F., Petit, M., Delsaut, N., Fortier, L., & Sempéré, R. 2012. Intense photooxidative degradation of planktonic and bacterial lipids in sinking particles collected with sediment traps across the Canadian Beaufort Shelf (Arctic Ocean). *Biogeosciences* 9(11): 4787-4802.

Rontani, J.-F., Belt, S. T., Brown, T. A., Amiraux, R., Gosselin, M., Vaultier, F., & Mundy, C. J. 2016. Monitoring abiotic degradation in sinking versus suspended Arctic sea ice algae during a spring ice melt using specific lipid oxidation tracers. *Org. Geochem*. 98: 82-97.

Rontani, J., & Belt, S. T. 2020. Photo- and autoxidation of unsaturated algal lipids in the marine environment: An overview of processes, their potential tracers, and limitations. *Org. Geochem*. 139: 103941.

Rontani, J.-F. 2021. Lipid Oxidation Products: Useful Tools for Monitoring Photo- and Autoxidation in Phototrophs. Cambridge Scholars Publishing, 178 pp.

Rontani, J.-F., Amiraux, R., Smik, L., Wakeham, S. G., Paulmier, A., Vaultier, F., Sun-Yong, H., Jun-oh, M., & Belt, S. T. 2021. Type II photosensitized oxidation in

senescent microalgal cells at different latitudes: Does low under-ice irradiance in Polar Regions enhance efficiency? *Sci. Tot. Environ*. 779: 146363.

Rontani J-F., Laslandes C., Vilgrain L., Vaultier, F. & Amiraux R. 2022. Control of the preservation of sympagic algal material in surficial sediments of central and eastern Baffin Bay by bactericidal hydroperoxides and free fatty acids. *Mar. Chem*. (Under review)

Sarra, A., di Bommarito, C., Anello, F., Iorio, T. D., Meloni, D., Monteleone, F., Pace, G., Piacentino, S., & Sferlazzo, D. 2019. Assessing the quality of shortwave and longwave Irradiance observations over the ocean: one year of high-time-resolution measurements at the Lampedusa oceanographic observatory. *J. Atmos. Ocean. Technol*. 36(12): 2383-2400.

Schaum, C. E. 2019. Enhanced biofilm formation aids adaptation to extreme warming and environmental instability in the diatom *Thalassiosira pseudonana* and its associated bacteria. *Limnol. Oceanogr*. 64(2): 441-460.

Sicre, M.-A., Paillasseur, J.-L., Marty, J.-C., & Saliot, A. 1988. Characterization of seawater samples using chemometric methods applied to biomarker fatty acids. *Org. Geochem.* 12(3): 281-288.

Skovsen, E., Snyder, J. W., Lambert, J. D. C., & Ogilby, P. R. 2005. Lifetime and Diffusion of Singlet Oxygen in a Cell. *J. Phys. Chem. B*, 109(18): 8570-8573.

Zolla, L. & Rinalducci, S. 2002. Involvement of active oxygen species in degradation of light-harvesting proteins under light stresses. *Biochemistry* 41: 14391-14402.

FIGURE CAPTIONS

Fig. 1. Map showing the location of the different stations investigated. Sinking particles were collected in open water, first-year ice, and marginal ice zones in Beaufort Sea, Resolute Passage and central Baffin Bay, respectively. Sea ice samples originated from Davis Strait.

Fig. 2. Measurement of vaccenic acid photooxidation products in *P. stutzeri* cultures with and without addition of *Thalassiosira* sp. cells after irradiation (1000 KJ.m^{-2}) under low PAR, high PAR and high PAR+UV irradiances (n=3).

Fig. 3. Conceptual scheme of the effect of $^1O_2$ on bacteria attached to senescent phytoplankton cells under low or high irradiance.

Fig. 4. Values of the ratio of % vaccenic acid photooxidation to % palmitoleic acid photooxidation in particulate matter samples collected in the Arctic under different irradiance conditions (A) and in sea-ice samples collected at the GreenEdge 2016 ice camp (B). Kruskal-Wallis test,

p-values : 0 < "***" < 0.001 < "**" < 0.01 < "*" < 0.05 < " "

Fig. S1. MRM chromatograms (with the transitions *m/z* 357 → 129 and *m/z* 199 → 129) showing the production of significant proportions of 12-hydroxyoctadec-10(*cis*)-enoic and 11-hydroxyoctadec-12(*cis*)-enoic acids (indicative of an effect of UV radiation, Christodoulou et al., 2010), respectively, after irradiation of *Thalassiosira* sp. cells associated with *P. stutzeri* under high solar irradiance (500 W.m^{-2}) for 3h 30.

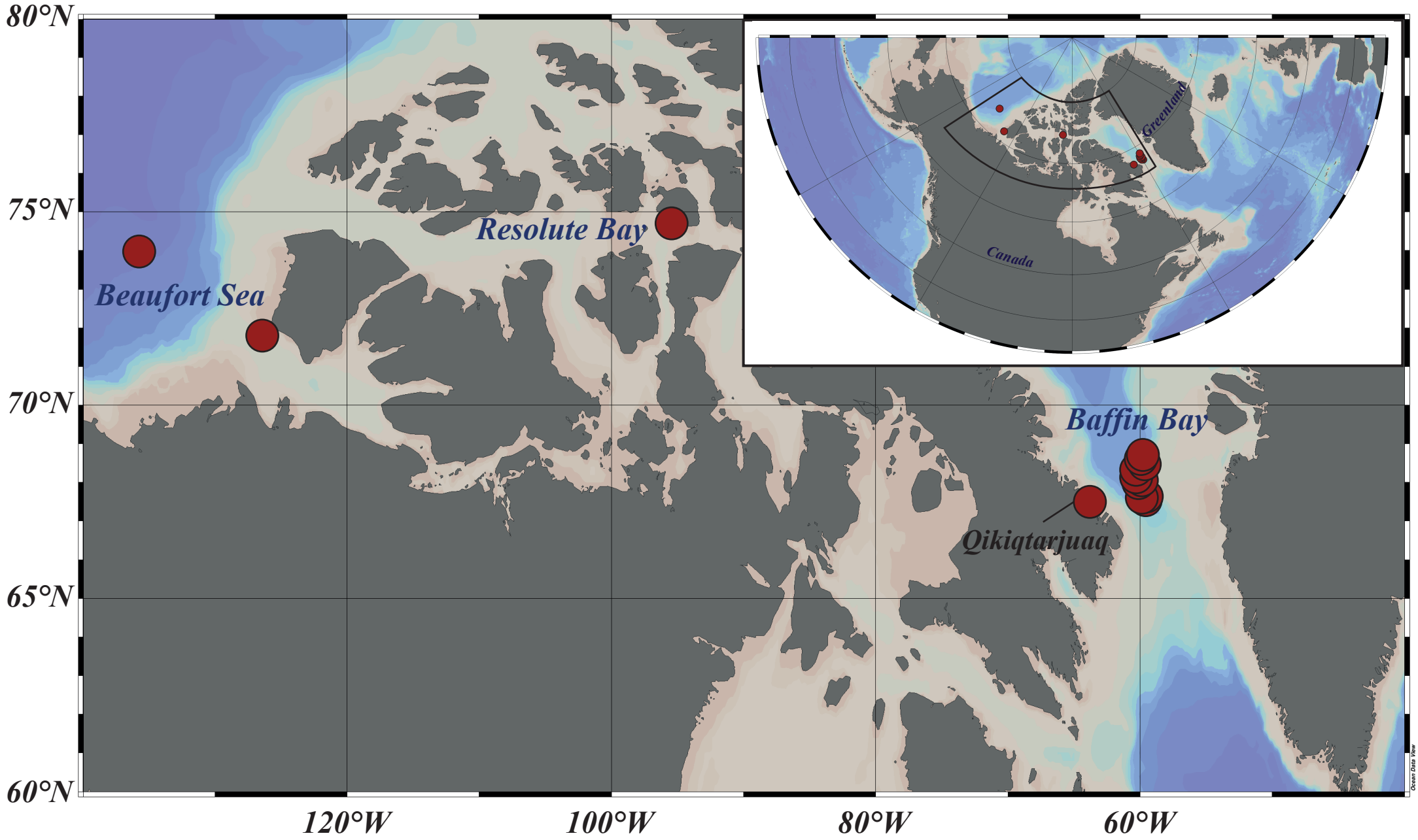
80°N
75°N
70°N
65°N
60°N
120°W
100°W
80°W
60°W
Beaufort Sea
Resolute Bay
Baffin Bay
Qikiqtarjuaq
Canada
Greenland
Ocean Data View

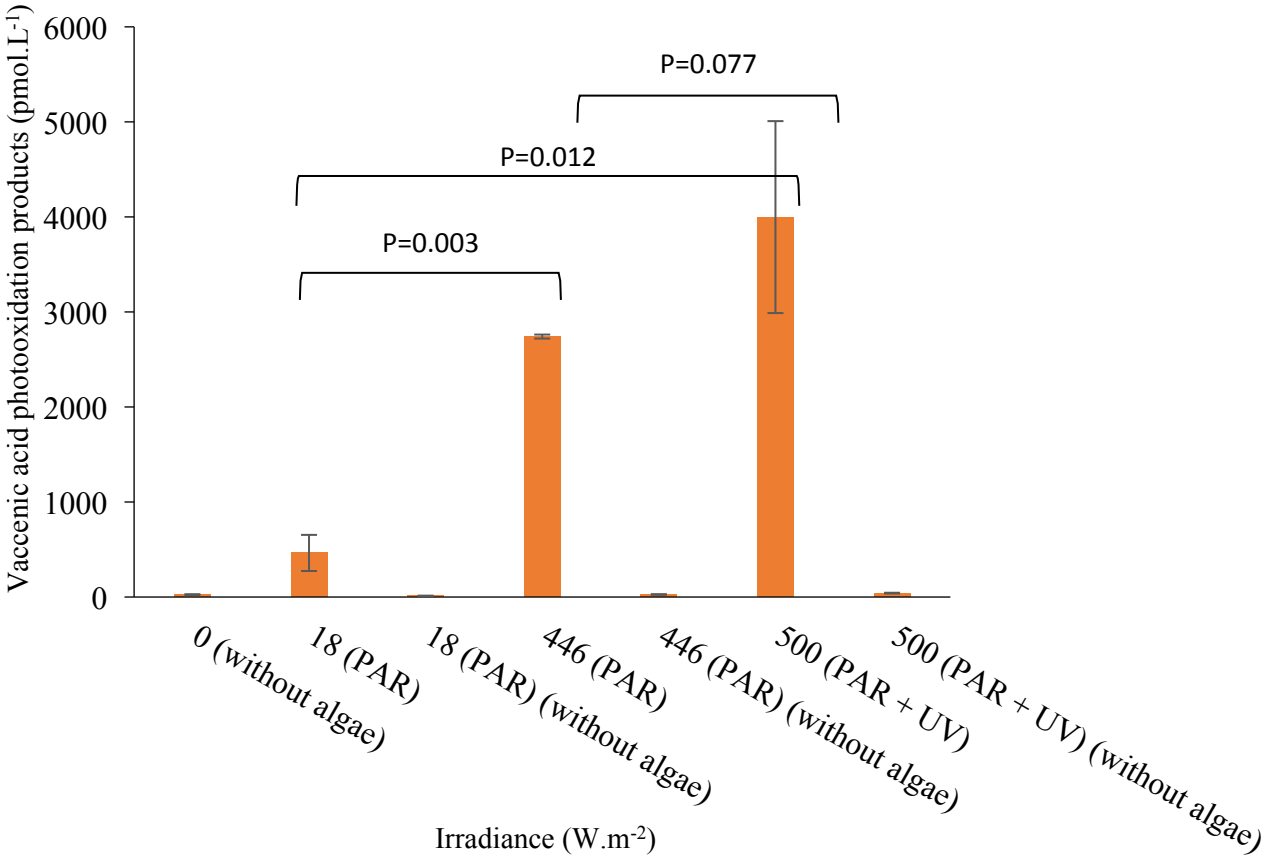
Vaccenic acid photooxidation products (pmol.L-1)
6000
5000
4000
3000
2000
1000
0
P=0.077
P=0.012
P=0.003
0 (without algae)
18 (PAR)
18 (PAR) (without algae)
446 (PAR)
446 (PAR) (without algae)
500 (PAR + UV)
500 (PAR + UV) (without algae)
Irradiance (W.m-2)

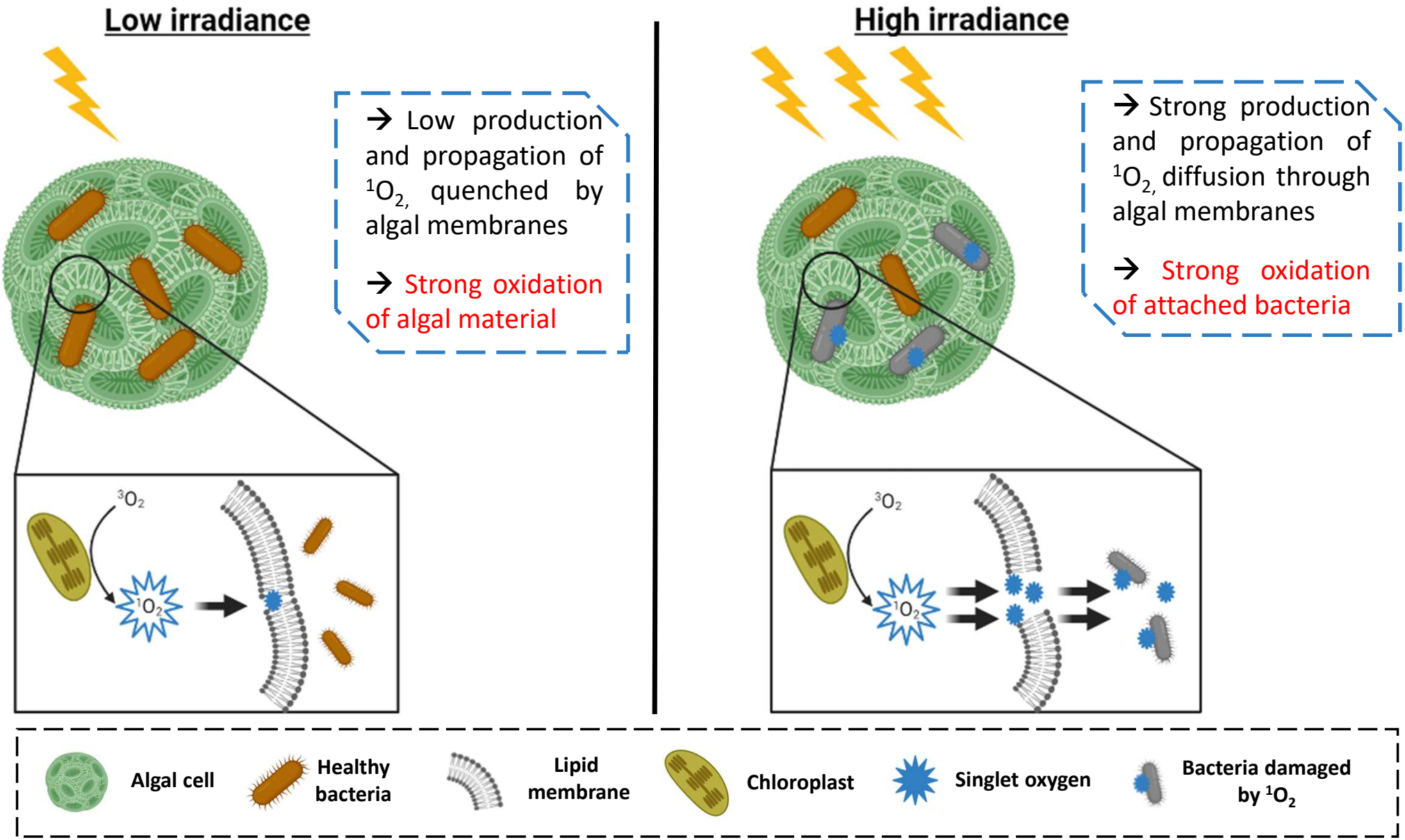
Low irradiance
→ Low production and propagation of $^1O_2$, quenched by algal membranes
→ Strong oxidation of algal material
$^3O_2$
$^1O_2$
High irradiance
→ Strong production and propagation of $^1O_2$, diffusion through algal membranes
→ Strong oxidation of attached bacteria
$^3O_2$
$^1O_2$
Algal cell
Healthy bacteria
Lipid membrane
Chloroplast
Singlet oxygen
Bacteria damaged by $^1O_2$

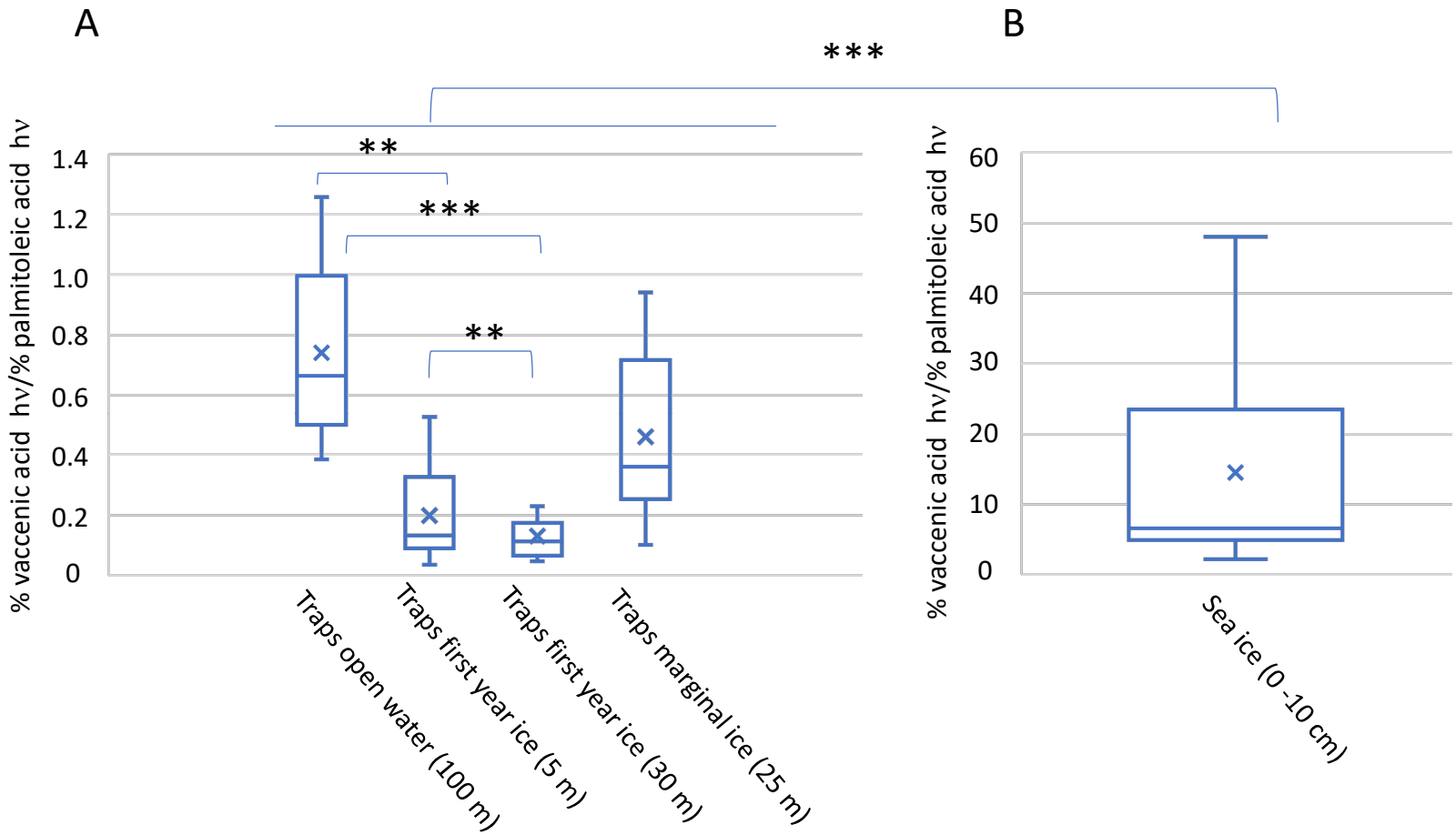
A
B
***
**
***
**
% vaccenic acid hv/% palmitoleic acid hv
1.4
1.2
1.0
0.8
0.6
0.4
0.2
0
Traps open water (100 m)
Traps first year ice (5 m)
Traps first year ice (30 m)
Traps marginal ice (25 m)
% vaccenic acid hv/% palmitoleic acid hv
60
50
40
30
20
10
0
Sea ice (0 -10 cm)

Table 1. Concentration of vaccenic acid photooxidation products in *P. stutzeri* cultures with and without addition of *Thalassiosira* sp. cells after irradiation (1000 KJ.m^{-2}) under low PAR, high PAR and high PAR+UV irradiances (n=3).

Irradiance (W m^{-2})	Vaccenic acid hv (pmol.L^{-1})[a]	Standard deviation
0 (without algae)	24	6
18 (PAR)	464	190
18 (PAR) (without algae)	13	0
446 (PAR)	2741	21
446 (PAR) (without algae)	27	3
500 (PAR + UV)	3998	1010
500 (PAR + UV) (without algae)	41	4

[a] Mean values.

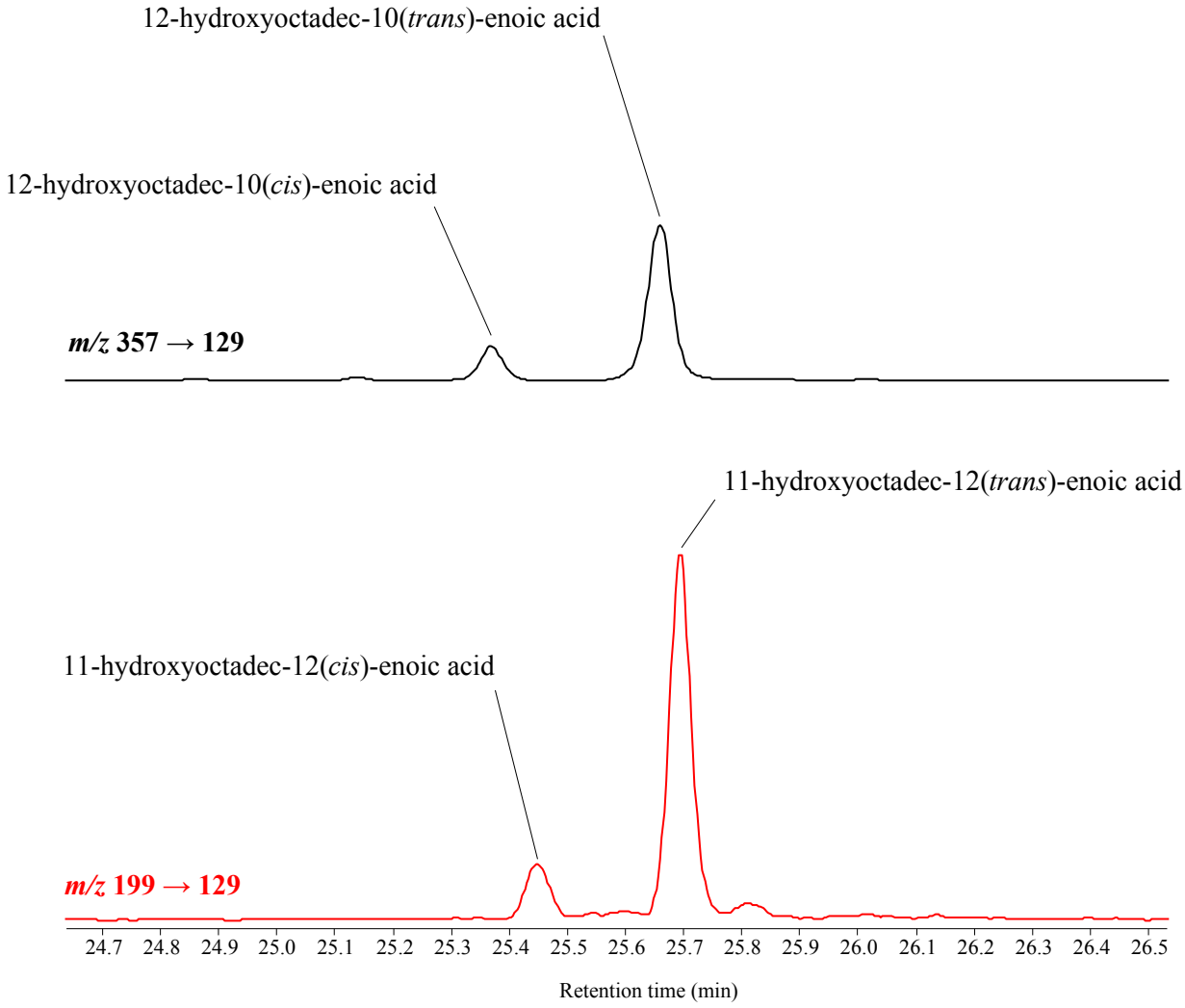
12-hydroxyoctadec-10(*trans*)-enoic acid
12-hydroxyoctadec-10(*cis*)-enoic acid
***m/z* 357 → 129**
11-hydroxyoctadec-12(*trans*)-enoic acid
11-hydroxyoctadec-12(*cis*)-enoic acid
***m/z* 199 → 129**
24.7 24.8 24.9 25.0 25.1 25.2 25.3 25.4 25.5 25.6 25.7 25.8 25.9 26.0 26.1 26.2 26.3 26.4 26.5
Retention time (min)

Table S1: Significant differences between % vaccenic acid photooxidation to % palmitoleic acid photooxidation ratios measured in the Arctic under different irradiances (P-Values, n = 3, KW test)

	Traps under open water (100 m) Malina	Traps under first year ice (5 m) (Resolute Passage)	Traps under first year ice (30 m) Resolute passage	Traps under marginal ice zone (30 m) Baffin Bay	Sea ice
Traps under open water (100 m) Malina	1	0,005	0,000	0,109	0,001
Traps under first year ice (5 m) (Resolute Passage)	0,005	1	0,997	0,111	0,002
Traps under first year ice (30 m) Resolute passage	0,000	0,997	1	0,004	0,001
Traps under marginal ice zone (30 m) Baffin Bay	0,109	0,111	0,004	1	0,001
Sea ice	0,001	0,002	0,001	0,001	1